JCTC Journal of Chemical Theory and Computation

ARTICLE

pubs.acs.org/JCTC

Solvation Effects on Electronic Transitions: Exploring the Performance of Advanced Solvent Potentials in Polarizable Embedding Calculations

Tobias Schwabe,*[,†] Jógvan Magnus Haugaard Olsen,[‡] Kristian Sneskov,[†,§] Jacob Kongsted,[‡] and Ove Christiansen[†,§]

[†]Center for Oxygen Microscopy and Imaging, Department of Chemistry, Aarhus University, Langelandsgade 140, DK-8000 Aarhus C, Denmark

[‡]Department of Physics and Chemistry, University of Southern Denmark, Campusvej 55, DK-5230 Odense M, Denmark

[§]The Lundbeck Foundation Center for Theoretical Chemistry, Department of Chemistry, Aarhus University, Langelandsgade 140, DK-8000 Aarhus C, Denmark

Supporting Information

ABSTRACT: The polarizable embedding (PE) approach, which combines quantum mechanics (QM) and molecular mechanics (MM), is applied to predict solvatochromic effects on excitation energies of several representative molecules in aqueous, methanol, acetonitrile, and carbon tetrachloride solutions. Good agreement with experimental results for excitation energies and for solvatochromic shifts is demonstrated on the basis of either density functional theory or coupled cluster methods. Solvent-dependent trends are fully reproduced in this diverse set of solvents. Furthermore, it is shown that the inclusion of higher order multipole moments and anisotropic polarizabilities in the electrostatic embedding potentials leads to a faster convergence with respect to a full QM treatment (within about 0.1 eV of estimated full QM treatments). It is thereby illustrated that the use of advanced solvent potentials can provide higher accuracy compared to various simpler approaches for the prediction of solvent shifts and do so in a computationally competitive manner.

1. INTRODUCTION

Quantum chemistry has developed a thorough knowledge about isolated molecules in vacuum at 0 K. Over the years, many theoretical methods have been developed and benchmarked for performance in different contexts. As a result, methods with known accuracy and computational cost exist for attacking a variety of chemical problems . These methods are primarily grounded in density functional theory (DFT) and post-Hartree−Fock wave function approaches, and benchmarking is an active field in (vacuum) quantum chemistry.[1−4] However, this picture changes when we turn to condensed phases in general and to solvation in particular. Here, the computational demands increase due to a number of factors: the system size increases rapidly because of the long-range Coulombic interactions, and dynamical effects need to be taken into account due to nonzero temperature effects. Therefore, more often than not, solvation studies have been addressed within the framework of molecular mechanics. Indeed, good results have been reported in the simulation of macroscopic properties.[5] However, when properties directly related to the electronic structure are the focus, it is necessary to go beyond a completely classical description. One very obvious case for this is the calculation of electronic excitations due to light absorption.

To be able to treat these processes, one may rely on hybrid approaches like combined quantum mechanics and molecular mechanics (QM/MM).[6] Here, the system is divided into a quantum mechanical subsystem (QM), where the excitation takes place, and the surrounding environment (MM), which is normally described by the electrostatic potentials of discrete solvent molecules. Alternatively, the bulk solvent effects can be described with an implicit solvation model like the conductor-like solvation model (COSMO)[7,8] or the polarizable continuum model (PCM).[9−11] Recently, a combination of QM/MM and PCM (the QM/MM/PCM model) has also been put forward for the calculation of electronic excitation energies in condensed phases.[12] While the gain in computation cost with an implicit solvation model is considerable, solvent-specific effects are not covered well.[13] In particular, the effect of hydrogen bonding is not well reproduced. A further drawback of an implicit approach is that it is not straightforward to extend to other similar molecular systems where QM/MM approaches, on the other hand, have proven beneficial, e.g., for the study of large biomolecular systems.[14] However, applying explicit solvent approaches for the description of solvation effects on excitation energies is a complex task. Due to temperature effects, it is necessarry to sample the configurational space of the solute−solvent system. For this, a molecular dynamics (MD) or Monte Carlo (MC) simulation approach is needed. This may be carried out in a pure MM or a QM/MM framework. Furthermore, within the past decade, full ab initio MD simulations in the framework of Car−Parrinello MD (CPMD) have become feasible.[15] Recently,

Received: April 15, 2011
Published: May 23, 2011

other schemes and combinations thereof have been developed and applied.[16−19] The MD simulation yields many molecular configurations (often more than 100), all of which have to be subjected to a QM/MM calculation of the electronic excitation energy. Therefore, the quality of the solvent description relies on the quality of the underlying MD simulation, the QM method, the potentials used in the MM part, and the coupling of the QM and MM subsystems. In fact, a further practical complication arises because, normally, depending on the chosen combination for QM/MM, there are no integrated programs carrying out the full protocol.

Overall, there is a need for more accurate QM/MM methods. This requires an improvement of all relevant components in order to increase the overall accuracy. While a lot of effort has been spent to make more accurate QM methods available for QM/MM treatments, the description of the MM subsystem has received less attention. To address the former, a coupled cluster (CC) as well as a DFT QM/MM approach with polarizable force fields have been introduced.[20−22] Furthermore, redesigned implementations of both approaches have recently been presented using a polarizable embedding (PE) scheme,[23,24] adding, among other things, the possibility to use multipole moments up to octopoles as well as anisotropic polarizabilities to describe the electrostatic embedding potential.

We emphasize that the PE approach to QM/MM studied here uses a fully self-consistent description of the polarization between the QM (be it DFT or CC) and MM subsystems, for both the ground and excited states. The need for a balanced description of the polarization when investigating solvation effects was recognized 15 years ago by Thompson, who introduced a QM/MM scheme using polarizable force fields and a semiempirical QM method.[25] The pioneering work for QM/MM by Warshel and Levitt[6] also considered mutual polarization of both subsystems. Other approaches in that direction include an alternative implementation of DFT/MM using polarizable force fields,[26,27] frozen-density embedded density functional theory,[28,29] the effective fragment potential approach,[30−32] CASPT2/MM using polarizable force fields,[33] and the many-body expansion scheme.[34] The PE scheme differs from other embedding schemes in that it is derived from a long-range perturbational analysis of interacting subsystems. The most important of these effects are then described combining a full quantum description of one part of the full system, with an essentially electrostatic description of the remaining parts and their interaction with the electronic QM system. Therefore, in its present form, the PE scheme does not take into account short-range and dispersion effects on the electronic wave functions and energies, which are of a pure quantum mechanical nature. For further comparison between different embedding schemes, we refer to the literature.[35]

An important reason for using sophisticated electrostatic potentials is that, in principle, this will allow accurate mimicking of the effects of hydrogen bonding to the QM system. Hence, one avoids the need of including the closer lying solvent molecules in the QM region. Especially for CC methods, the gain in computational efficiency is formidable and may be regarded as a prerequisite for applying CC methods routinely for QM/MM studies. Thorough treatment of hydrogen bonding is also mandatory for QM/MM studies of biomolecular systems where the border between the QM and MM region is often across hydrogen bonds. Advanced electrostatic potentials could provide higher accuracy compared to simpler approaches since, aiming for a given accuracy, the inclusion of selected parts of the environment into the QM calculations should be far less important. However, these considerations are rather general and at least partially lack numerical evidence. In this paper, we present benchmark calculations that demonstrate how accurate solvatochromic shifts for electronic excitation energies can be obtained for a range of different solvents by applying the PE model in conjunction with electrostatic potentials derived from ab initio calculations. It is shown that the accuracy can be improved systematically by inclusion of higher order multipoles and polarizabilities in the electrostatic potential. We illustrate how these enhanced electrostatic potentials indeed significantly reduce the importance of including the nearest solvent molecules in the QM region while still yielding accurate results.

2. THEORY

In the following, we restrict ourselves to a brief introduction of the electronic QM/MM interface in the PE approach. A detailed derivation of ground state energy and response function expressions for DFT and CC can be found elsewhere.[23,24] The general idea of the PE model is an expansion of the surrounding charge density in classical terms at discrete expansion points. The atomic sites of the MM region are an obvious choice for the expansion points, but bond midpoints can also be included. Each expansion point may be described by localized multipole moments (up to octopoles) and an anisotropic (or isotropic) polarizability which allows for dipole−dipole polarization. From this, we obtain an electrostatic ($E_{\mathrm{PE}}^{\mathrm{es}}$) and polarization (or induction; $E_{\mathrm{PE}}^{\mathrm{pol}}$) energy contribution. The former is given by the interaction between the permanent multipole moments in the MM region and the electrons and nuclei in the QM region:

$$E_{\mathrm{PE}}^{\mathrm{es}} = \sum_{s=1}^{S}\sum_{k=0}^{K}\frac{(-1)^k}{k!}\left(\sum_{m=1}^{M} Z_m \mathbf{T}_{ms}^{(k)} - \sum_{i=1}^{N}\mathbf{T}_{is}^{(k)}\right)\mathbf{Q}_s^{(k)} \quad (1)$$

Here, S is the total number of expansion points s, M is the number of QM nuclei m, with nuclear charges Z_m, and N is the number of electrons i. The interaction tensors $\mathbf{T}_{st}^{(k)}$ are defined as

$$\mathbf{T}_{st}^{(k)} = \nabla_s^k \frac{1}{(|\mathbf{r}_s - \mathbf{r}_t|)} \quad (2)$$

where ∇_s is a derivative operator with respect to coordinates r_s. $\mathbf{Q}_s^{(k)}$ is a multipole moment of kth order located at expansion point s; i.e., for $k = 0$, it is a point charge; for $k = 1$, a dipole moment; and so on.

The polarization energy due to the mutual polarization between the environment and QM region is given by

$$E_{\mathrm{PE}}^{\mathrm{pol}} = -\frac{1}{2}\mu^{\mathrm{ind}}(\mathbf{F}^{\mathrm{nuc}} + \mathbf{F}^{\mathrm{elec}} + \mathbf{F}^{\mathrm{mul}}) = -\frac{1}{2}\mu^{\mathrm{ind}}\mathbf{F} \quad (3)$$

where the vector μ^{ind} of length $3S$ contains the complete set of induced dipoles. $\mathbf{F}$ is the electric field vector containing the fields from the nuclei, electrons, and multipole moments in the MM region. To obtain the induced dipoles, one has to include the mutual interaction with the electric fields from all other induced dipoles and from the static electric field. This can be cast into a matrix equation

$$\mu^{\mathrm{ind}} = \mathbf{R}(\mathbf{F}^{\mathrm{nuc}} + \mathbf{F}^{\mathrm{elec}} + \mathbf{F}^{\mathrm{mul}}) = \mathbf{RF} \quad (4)$$

where **R** is a symmetric classical response matrix of dimension $3S \times 3S$. It is defined as

$$\mathbf{R} = \begin{pmatrix} \alpha_1^{-1} & \mathbf{T}_{12}^{(2)} & \cdots & \mathbf{T}_{1S}^{(2)} \\ \mathbf{T}_{21}^{(2)} & \alpha_2^{-1} & \ddots & \vdots \\ \vdots & \ddots & \ddots & \mathbf{T}_{(S-1)S}^{(2)} \\ \mathbf{T}_{S1}^{(2)} & \cdots & \mathbf{T}_{S(S-1)}^{(2)} & \alpha_S^{-1} \end{pmatrix}^{-1} \quad (5)$$

The inverse of the polarizability tensors α_s are placed along the diagonal, while the dipole−dipole interaction tensors are found as off-diagonal elements. An effective operator which couples the QM system and the environment can be derived from the presented energy expressions and further generalized to the calculation of, e.g., vertical electronic excitation energies within the framework of linear response theory. For details concerning the DFT (Hartree−Fock) or CC implementation of the PE model, we refer to the literature.[23,24]

3. COMPUTATIONAL DETAILS

In the following, we describe the procedure used to compute the solvatochromic effects. The general concept follows the sequential Monte Carlo and QM (S-MC/QM) approach introduced by Coutinho and Canuto.[36] A classical MD simulation for the solute in solvation is carried out. From this simulation, we obtain a set of molecular configurations which are treated at a higher level of theory to calculate excitation properties of the system. The configurations are obtained from a thermally coupled simulation, and therefore they already inherit a Boltzmann distribution weighting. Thus, the properties of interest can be calculated directly as the average over all configurations. In principle, further information can be gained on the basis of the distribution of the property values.

Unless otherwise noted, the properties in solution are obtained by averaging over 120 snapshots of an MD simulation (see below). To save computational resources, in some cases, only 30 configurations have been used. To indicate the quality of the averaged results, we report the standard error of the mean (SEM). The effect of using only one-fourth of the configurations does not influence the results significantly. The difference between values averaged from 30 or 120 configurations is about 0.01 eV and therefore well below other effects like basis set incompleteness, the level of theory, or the approximations of the electrostatic environment.

3.1. Potential Determination. The multipole moments and polarizabilities are all obtained in the same way for solutes as well as solvents. First, the molecules are optimized at the B3LYP[37,38]/aug-cc-pVTZ[39,40]/PCM[9,10] level of theory, where we apply the standard PCM parameters as provided in Gaussian 09.[41] Next, we determine the multipole moments up to octopoles as well as the anisotropic polarizabilities by applying the LoProp[42] approach as implemented in MOLCAS.[43] The properties are calculated at the B3LYP/a-aug-cc-pVTZ[39,40] level for the isolated molecules in a vacuum using the geometry obtained from the PCM optimization. The a-aug-cc-pVTZ basis set is a recontraction of aug-cc-pVTZ to an ANO-type basis, which is necessary for the LoProp procedure.

Finally, we also obtain atomic point charges with the CHelpG procedure[44] fitted against the electrostatic potential from a B3LYP/aug-cc-pVTZ calculation again at the PCM optimized geometries. As an additional constraint, the reproduction of the molecular dipole moment is imposed on the fitting. These point charges implicitly contain higher order multipole effects and therefore cannot be combined with a rigorous multipole moment expansion. Thus, whenever we only use point charges, we use those obtained from the CHelpG fitting (except for the comparison of the potentials with their ab initio counterpart), and otherwise the LoProp point charges are used. It should be mentioned that the sole purpose of the potentials is to reproduce as accurate as possible the exact electrostatic environmental potential and its (direct) response to a change in the solute electron density. In the following, we identify different approximations to the electrostatic potential as follows: Mm labels the applied multipole moments, with $m = 0$, point charges; $m = 1$, up to dipoles; $m = 2$, up to quadrupoles; and $m = 3$, up to octopoles, and Pp labels the polarizability of the MM centers, with $p = 0$, no polarization; $p = 1$, isotropic polarizabilities; and $p = 2$, anisotropic polarizabilities. To identify fitted point charges, we use the label M*. All potentials which have been obtained for this study are listed in the Supporting Information.

3.2. Molecular Dynamic Simulations. For all simulations, an equilibration run of 0.4 ns in time steps of 2 fs followed by a production run of 1.2 ns is carried out. Configurations are sampled every 10 ps. This time step is considered sufficient to obtain statistically uncorrelated configurations. The NVT ensemble is applied with $T = 298$ K. All molecules are treated as rigid bodies. Thus, only intermolecular potentials are considered. These are based on a 12-6-Lennard-Jones potential and our M*P1 potentials. The construction of the M*P1 potentials is described in the previous section. The Lennard-Jones parameters are taken from the OPLS-AA force field[45] as shipped with TINKER.[46]

To model aqueous solutions, we used a slightly different potential, which consists of point charges and a molecular isotropic polarizability located at the oxygen atom, called the SPCpol water model.[47] This potential was used in all MDs of aqueous solutions. It was chosen to maintain comparability to previous studies. Note that we do not expect significant changes if the M*P1 potential for water had been applied instead. All simulations have been carried out with the MOLSIM program package.[48]

3.3. PE-QM Calculations. The PE-QM calculations are performed using either CAM-B3LYP[49]/aug-cc-pVDZ[39,40] or CCSD[50]/aug-cc-pVDZ for the QM part. Inputs are generated with the WHIRLPOOL program.[51] For each configuration, the solute geometry is extracted, and a cutoff radius of 12 Å from the center of mass of the solute is applied. All solvent molecules within the cutoff are included in the electrostatic embedding potential. The actual PE-QM computations are done with a development version of the DALTON program.[52] Excitation energies for which the PCM model has been applied are computed with Gaussian 09.[41] All PCM calculations are performed using default settings: atomic radii are taken from universal force field and scaled by 1.1, and the static/dynamic dielectric constants are 78.355/1.778 (water), 32.613/1.766 (methanol), 35.688/1.807 (acetonitrile), and 2.228/2.132 (carbon tetrachloride).

3.4. Solvent Potential Analysis. To analyze the quality of the solvent potentials used in this work, the electrostatic potentials due to the multipole moments are compared to a QM reference. The QM calculations are performed at the same level of theory and geometry as the corresponding calculation of the potential parameters, i.e., at the B3LYP/aug-cc-pVTZ level using the

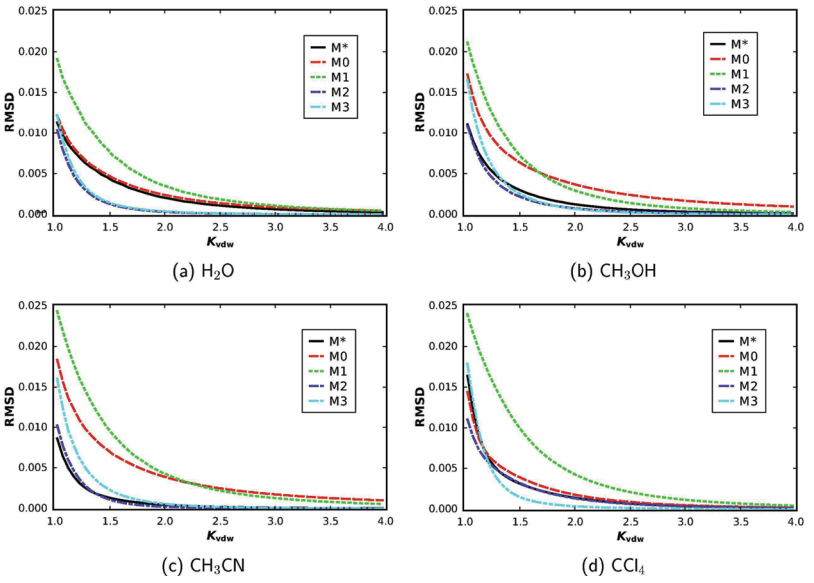

Figure 1. Plots of the RMSD in au between the electrostatic potentials created by permanent multipole moments and a QM reference with respect to distance from the molecular surface defined by interlocking atomic van der Waals spheres.

B3LYP/aug-cc-pVTZ/PCM geometry. For the analysis of the electrostatic potential due to induced dipole moments, we apply a static electric field in the *x*, *y*, and *z* directions with a magnitude of 0.01 au. The electrostatic potential is sampled at a number of points surrounding a single solvent molecule. The sampling volume consists of an inner boundary defined by interlocking atom-centered van der Waals spheres. The outer boundary is similarly defined using van der Waals spheres which have a radius of 4 times the van der Waals radii. The hydrogen van der Waals radius is from ref 53, and all other are from ref 54. Inside the volume, a number of points are uniformly distributed with a distance of 0.1 Å in the *x*, *y*, and *z* directions. This leads to 978 261, 1 343 269, 1 546 866, and 2 435 010 sampling points for water, methanol, acetonitrile, and carbon tetrachloride, respectively. In order to inspect the quality of the electrostatic potentials with respect to the distance from the molecule, we divide the entire volume into smaller subvolumes defined by an inner and outer boundary which is defined by van der Waals radius scaling factors, K_{vdw}, and calculate the root-mean-square deviation (RMSD) over all points inside each subvolume. Each subvolume has a thickness of $0.05K_{vdw}$. The root-mean-square deviation (RMSD) is calculated as

$$\mathrm{RMSD} = \sqrt{\frac{1}{N}\sum_{a}(\varphi_a^{\mathrm{es}} - \varphi_a^{\mathrm{QM}})^2} \qquad (6)$$

where *a* is a sampling point, *N* is the total number of sampling points, and φ_a^{es} and φ_a^{QM} are the electrostatic potentials at point *a* due to the solvent potential and the QM reference, respectively. In the case of induced dipoles, the QM reference potential is obtained by subtracting the unperturbed electrostatic potential from the potential obtained in the external field.

The grid generation and calculation of electrostatic potentials due to the multipoles is handled by the Whirlpool program. Whirlpool also creates the input necessary for the QM calculations which are carried out using the DALTON program. The subsequent comparisons between the electrostatic potentials are also performed using the Whirlpool program.

4. RESULTS AND DISCUSSION

4.1. Analysis of the Solvent Potentials. The quality of the solvent potentials, derived from the LoProp and CHelpG schemes, is evaluated by a comparison between the electrostatic potentials created by the multipole moments and the corresponding QM reference. The RMSDs between the electrostatic potentials with respect to the distance from the molecule are presented in Figure 1 in the case of permanent multipoles and Figure 2 in the case of induced dipoles.

The general observations for the permanent multipole moments derived from the LoProp procedure for all the considered solvents is that the electrostatic potential is reasonably well reproduced far away from the molecule, even at the lowest level, i.e., the M0 potential. However, as we approach midrange distances, the electrostatic potential due to M0 and M1 worsens, while the M2 and M3 potentials still retain good accuracy due to the higher order multipole moments. At short and especially very short range, the deviation from the QM reference increases rapidly for all potentials.

The M1 potential gives the poorest description in all cases, except at mid and long ranges for methanol and acetonitrile, where it performs slightly better than the M0 potential. We also observe that the general short-range performance of the M2 potential is better than or equal to the M3 potential. However, in the case of carbon tetrachloride, the M3 potential performs very well except at very short distances. Here, it is also worth noting that the M0 potential gives similar results to those of the M2 potential. The most noteworthy result is that the M* potential generates electrostatic potentials of almost the same quality as the M2 potential except for a water molecule. This is expected because the charges have been fitted against the QM electrostatic potential. The less accurate description for water can be explained by the fact that there are only three charges, which does not give enough flexibility

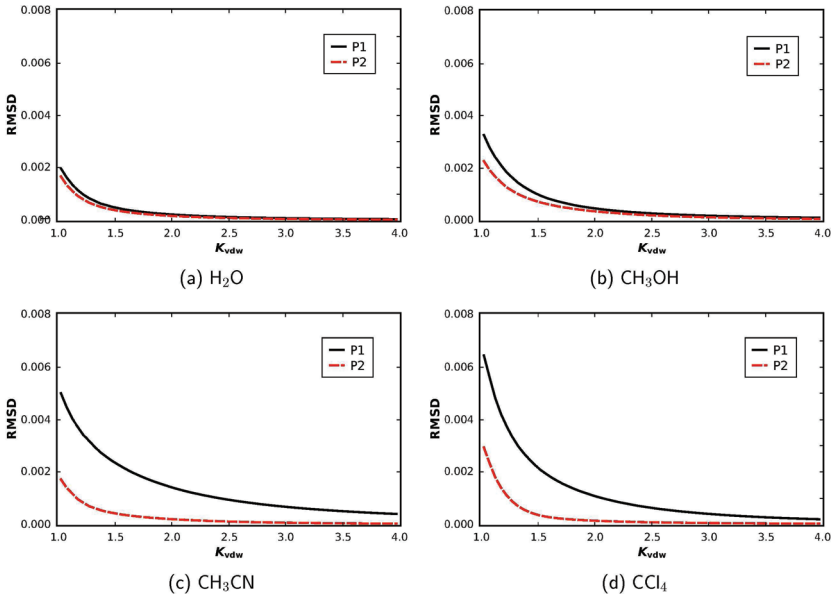

Figure 2. Plots of the RMSD in au between the induced electrostatic potentials created by induced dipole moments and a QM reference with respect to distance from the molecular surface defined by interlocking atomic van der Waals spheres.

Table 1. Excitation Energies (E^{exc}) and Shifts (Δ) for Acrolein in Water with PE-CAM-B3LYP/aug-cc-pVDZ and Different Numbers of Solvent Molecules (#QM-solv) Next to the Double Bond (C=C) or the Oxygen Atom (O) Included in the QM Region[a]

force field	#QM-solv (C=C)	#QM-solv (O)	E^{exc}		E^{exc}	
			($n-\pi^*$)	Δ^b	($\pi-\pi^*$)	Δ^b
TIP3P[c]	0	0	4.04	0.26	6.21	−0.20
M2P2	0	0	4.11	0.33	6.05	−0.36
M2P2	2	0	4.11	0.33	5.96	−0.45
M2P2	4	0	4.11	0.33	5.93	−0.48
M2P2	6	0	4.10	0.32	5.92	−0.49
M2P2	0	2	4.07	0.29	6.05	−0.36
M2P2	2	2	4.08	0.30	5.97	−0.44
M2P2	4	2	4.07	0.29	5.94	−0.47
M2P2	8	6	4.04	0.26	5.95	−0.46
exp[c]			3.94	0.25	5.90	−0.52

[a] Values are given in eV. All averaged excitation energies have a SEM of ±0.01. [b] Gas phase: CAM-B3LYP/aug-cc-pVDZ//B3LYP/aug-cc-pVTZ. [c] Taken from ref 55.

to reproduce higher order multipoles. Thus, only a marginally better description than with the M0 potential is achieved.

The quality of the polarizabilities is tested through the induced electrostatic potential created by induced dipoles generated by a static electric field. In general, we observe that the anisotropic polarizabilities, i.e., P2, give a better reproduction of the QM electrostatic potential than the isotropic polarizabilities, i.e., P1. However, for water and partly also methanol, the difference is less pronounced due to the overall lower magnitude of the polarizabilities of these molecules. The opposite is true in the case of acetonitrile and carbon tetrachloride, where we observe that the anisotropic polarizabilities perform much better—especially at short distances.

4.2. Acrolein in Water. A previous QM/MM study on acrolein solvated in water[55] revealed that even a point charge-and-polarizable potential (equivalent to M*P1 in our notation) was not sufficient to describe the solvatochromism of the two lowest excited states. Especially the $\pi-\pi^*$-transition suffered from an inadequate description of the environment, and the inclusion of 14 water molecules into the QM region was needed to achieve converged results. It has already been shown that the new PE-DFT approach remedies these shortcomings if higher multipoles and polarizabilities are taken into account (e.g., a M2P2 potential), and very good agreement with experimental results was obtained.[23] Here, we repeat the investigation of including solvent molecules into the QM region, now with the more advanced M2P2 potential, to investigate the convergence with respect to a full QM treatment. We use the same 120 configurations as in ref 55. Results are given in Table 1.

From this analysis, we first note that we approach the same limit for the excitation energies with an increasing number of QM water: 4.05 eV vs 4.04 eV (this study) for the $n-\pi^*$ state and 5.97 eV vs 5.95 eV (this study) for the $\pi-\pi^*$ state, although the previous study used the TIP3P water potential[56] for the MM region. This shows that we indeed approach the limit of a full QM treatment. Of course, 14 water molecules are not sufficient to describe bulk effects (and therefore the MM region cannot be neglected), but the numerical experiment shows that the long-range Coulomb effects can be modeled using simpler solvent potentials. This is consistent with the analysis of the solvent potentials in the previous section. Furthermore, we observe that the PE(M2P2)-CAM-B3LYP result without any QM treated solvent molecules is already within 0.1 eV of this limit, which halves the deviation for the $\pi-\pi^*$ excitation in comparison with the point charge only embedding. It should also be pointed out that, with the M2P2 potential, only two additional water molecules in the QM region are necessary to reproduce the limit of 14 water molecules. Depending on the excited state, these molecules have to be those closest to the oxygen atom or to the double bond. No significant additional improvement is obtained

Table 2. Excitation Energies for Acetone in Water with Respect to Different Force Fields for PE-QM Calculations with CAM-B3LYP (CB3) and CCSD (CC) and Different Numbers of Solvent Molecules (#QM-solv) Included in the QM Region[a]

		CB3		CC	
solv. model	#QM-solv	$E^{exc}(n-\pi^*)$	Δ^b	$E^{exc}(n-\pi^*)$	Δ^c
PCM	0	4.59	0.08		
M*P0	0	4.60 ± 0.01	0.09	4.66 ± 0.01[d]	0.08
M2P0	0	4.63 ± 0.02[d]	0.12	4.69 ± 0.02[d]	0.11
M*P2	0	4.69 ± 0.02[d]	0.18	4.75 ± 0.02[d]	0.17
M2P2	0	4.75 ± 0.02	0.24	4.80 ± 0.03[d]	0.22
M3P2	0	4.74 ± 0.01	0.23		
M2P2	1	4.70 ± 0.01	0.19		
M2P2	2	4.68 ± 0.01	0.17		
exp[e]		4.68	0.22		

[a] The aug-cc-pVDZ basis set was used. Excitation energies ($E^{exc}(n-\pi^*)$) and shifts (Δ) are given in eV and are averaged over 120 configurations, except where it is noted otherwise. [b] Gas phase: CAM-B3LYP/aug-cc-pVDZ//B3LYP/aug-cc-pVTZ. [c] Gas phase: CCSD/aug-cc-pVDZ//B3LYP/aug-cc-pVTZ. [d] Based on 30 configurations. [e] Taken from ref 57.

Table 3. Excitation Energies for Acetone in Methanol with Respect to Different Force Fields for PE-QM Calculations with CAM-B3LYP (CB3) and CCSD (CC) and Different Numbers of Solvent Molecules (#QM-solv) Included in the QM Region[a]

		CB3		CC	
solv. model	#QM-solv	$E^{exc}(n-\pi^*)$	Δ^b	$E^{exc}(n-\pi^*)$	Δ^c
PCM	0	4.59	0.08		
M*P0	0	4.55 ± 0.00	0.04	4.60 ± 0.01[d]	0.02
M2P0	0	4.54 ± 0.01[d]	0.03	4.60 ± 0.01[d]	0.02
M*P2	0	4.61 ± 0.02[d]	0.10	4.66 ± 0.02[d]	0.08
M2P2	0	4.64 ± 0.01	0.13	4.67 ± 0.02[d]	0.09
M3P2	0	4.63 ± 0.01	0.12		
M2P2	1	4.60 ± 0.01	0.09		
M2P2	2	4.60 ± 0.01	0.09		
exp[e]		4.58	0.12		

[a] The aug-cc-pVDZ basis set was used. Excitation energies ($E^{exc}(n-\pi^*)$) and shifts (Δ) are given in eV and are averaged over 120 configurations, except where it is noted otherwise. [b] Gas phase: CAM-B3LYP/aug-cc-pVDZ//B3LYP/aug-cc-pVTZ. [c] Gas phase: CCSD/aug-cc-pVDZ//B3LYP/aug-cc-pVTZ. [d] Based on 30 configurations. [e] Taken from ref 57.

Table 4. Excitation Energies for Acetone in Acetonitrile with Respect to Different Force Fields for PE-QM Calculations with CAM-B3LYP (CB3) and CCSD (CC) and Different Numbers of Solvent Molecules (#QM-solv) Included in the QM Region[a]

		CB3		CC	
solv. model	#QM- solv	$E^{exc}(n-\pi^*)$	Δ^b	$E^{exc}(n-\pi^*)$	Δ^c
PCM	0	4.59	0.08		
M*P0	0	4.52 ± 0.00	0.01	4.59 ± 0.01[d]	0.01
M2P0	0	4.52 ± 0.01[d]	0.01	4.58 ± 0.01[d]	0.00
M*P2	0	4.55 ± 0.01[d]	0.04	4.61 ± 0.01[d]	0.03
M2P2	0	4.55 ± 0.00	0.04	4.60 ± 0.01[d]	0.02
M3P2	0	4.54 ± 0.00	0.03		
M2P2	1	4.54 ± 0.00	0.03		
M2P2	2	4.53 ± 0.00	0.02		
exp[e]		4.52	0.06		

[a] The aug-cc-pVDZ basis set was used. Excitation energies ($E^{exc}(n-\pi^*)$) and shifts (Δ) are given in eV and are averaged over 120 configurations, except where it is noted otherwise. [b] Gas phase: CAM-B3LYP/aug-cc-pVDZ//B3LYP/aug-cc-pVTZ. [c] Gas phase: CCSD/aug-cc-pVDZ//B3LYP/aug-cc-pVTZ. [d] Based on 30 configurations. [e] Taken from ref 57.

Table 5. Excitation Energies for Acetone in Carbon Tetrachloride with Respect to Different Force Fields for PE-QM Calculations with CAM-B3LYP (CB3) and CCSD (CC) and Different Numbers of Solvent Molecules (#QM-solv) Included in the QM Region[a]

		CB3		CC	
solv. model	#QM- solv	$E^{exc}(n-\pi^*)$	Δ^b	$E^{exc}(n-\pi^*)$	Δ^c
PCM	0	4.52	0.01		
M*P0	0	4.46 ± 0.00	−0.05	4.53 ± 0.00[d]	−0.05
M2P0	0	4.45 ± 0.00[d]	−0.06	4.52 ± 0.00[d]	−0.06
M*P2	0	4.48 ± 0.00[d]	−0.03	4.55 ± 0.00[d]	−0.04
M2P2	0	4.47 ± 0.00	−0.04	4.54 ± 0.00[d]	−0.05
M3P2	0	4.48 ± 0.00	−0.03		
M2P2	1	4.47 ± 0.00	−0.04		
M2P2	2	4.46 ± 0.00	−0.05		
exp[e]		4.43	−0.03		

[a] The aug-cc-pVDZ basis set was used. Excitation energies ($E^{exc}(n-\pi^*)$) and shifts (Δ) are given in eV and are averaged over 120 configurations, except where it is noted otherwise. [b] Gas phase: CAM-B3LYP/aug-cc-pVDZ//B3LYP/aug-cc-pVTZ. [c] Gas phase: CCSD/aug-cc-pVDZ//B3LYP/aug-cc-pVTZ. [d] Based on 30 configurations. [e] Taken from ref 57.

by the successive inclusion of more molecules. This is in contrast to the TIP3P case where a monotonic convergence with an increasing QM region was observed for the $\pi-\pi^*$ state.[55] In passing, we note the good agreement of PE-CAM-B3LYP results with experimental results for the excitation energies as well as for the solvatochromic shifts.

4.3. Solvatochromism in Acetone. Encouraged by the good results of the PE model for water as the solvent, we investigated its applicability to other solvents. For this purpose, we examined the lowest excitation of acetone in water, methanol, acetonitrile, and carbon tetrachloride following the same procedure as outlined before. The data are extended by the inclusion of octopole moments in the solvent potentials and the use of PE-CCSD.

The results are given in Tables 2−5. Recent experimental[57] and calculated PCM-DFT values are also listed for comparison. The general trends are solvent-independent. Good results with respect to experimental results are achieved using PE-CAM-B3LYP at the M2P2 level with deviations for excitation energies below 0.1 eV and for solvatochromic shifts of only 0.02 eV or less. Thereby, the largest blue shift found in water (experimental, 0.22 eV; M2P2, 0.24 eV) and the red shift in CCl_4 (experimental, −0.03 eV; M2P2, −0.04 eV) are predicted correctly. The application of multipoles of higher order than quadrupole

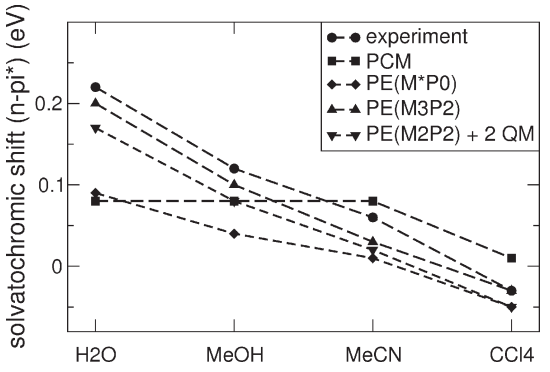

Figure 3. Solvatochromic shifts for the first $n-\pi^*$ electronic excitation energy of acetone. Theoretical results are based on CAM-B3LYP/aug-cc-pVDZ computations with the specified environment model (PCM or PE).

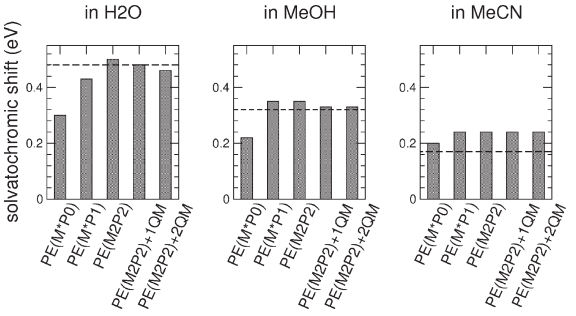

Figure 4. Solvatochromic shifts for the first $n-\pi^*$ electronic excitation energy of pyridazine in different solvents. Theoretical results are based on CAM-B3LYP/aug-cc-pVDZ computations and the indicated polarizable embedding potentials. Experimental results (taken from ref 58) are given as a dashed line.

moments in the electrostatic potential has no significant effect. The inclusion of solvent molecules in the QM region does not increase the quality of the $n-\pi^*$ state description. The PE-CAM-B3LYP results are in close correspondence with the PE-CCSD results, which yield slightly higher excitation energies (about 0.05 eV), but the shifts are almost identical.

Finally, a remark about the application of PCM-TDDFT is needed. One can argue that the results for the excitation energies are in an acceptable agreement with experimental results (all within 0.1 eV). However, relative shifts due to the solvent are as important as absolute excitation energies when solvatochromism is considered. In Figure 3, the shifts in different solvents obtained from the experiment as well as from some theoretical methods are shown. Clearly, PCM-TDDFT cannot reproduce this trend and is therefore not sufficient to describe relative shifts between different solvents. As expected, the deviations are largest for water and methanol where hydrogen bonds play a crucial role. These effects are not described at a sufficient level of theory by the PCM treatment. PCM also does not predict a red shift in CCl_4. For a more extensive discussion about the short-comings of (standard) continuum solvation models to describe the relative solvation shifts in acetone, see ref 13.

The trend of the solvatochromic shifts is improved by using a discrete solvation description, as can be seen from the PE(M*P0) results, but still deviates from what is found in the experiment. When polarization and higher multipoles are taken into account, very good agreement with experimental findings is achieved.

4.4. Solvatochromism in Pyridazine. To present an alternative case, we also calculated the solvatochromic shift of pyridazine in water, methanol, and acetonitrile. We limited the study to the M*P0, M*P1, and M2P2 potentials. For the M2P2 potential, up to two solvent molecules have been included in the QM region. The shifts are shown in Figure 4. Additionally, all excitation energies are listed in the Supporting Information.

The findings are very similar to those from the study of acetone. Convergence of the results is reached at the M2P2 level, and the computed shifts are in good agreement with experimental measurements (within 0.07 eV), while the deviation at the M*P0 level can be as high as 0.17 eV. The absolute excitation energies are about 0.1 eV too high compared to experimental results (see the Supporting Information), but some level of disagreement of the absolute excitation energy is to be expected given the after-all limited accuracy of the QM method, i.e., the CAM-B3LYP functional, as well as the neglect of nuclear relaxation and vibrational effects on the spectral profile. For acetonitrile, the difference between the M*P0 and M2P2 levels is least pronounced. Note that the agreement between experimental results and PE-CAM-B3LYP using the M*P0 potential is marginally better than that with the M2P2 potential, but the opposite is true with respect to the inclusion of solvent molecules in the QM region. However, effects are small, and the correct relative trend compared to water and methanol is obtained. In a previous study by one of us regarding the solvent shift in pyridazine in aqueous solution based on the SPCpol potential, which is similar to M*P1, it was found that the QM treatment of the two nearest water molecules is necessary to achieve a satisfying description of the solvent effects.[59] However, according to our observations, this is not necessary when using the M2P2 potential. Again, this finding is transferable to the other solvent potentials.

5. SUMMARY AND CONCLUSION

The polarizable embedding approach to the QM/MM description of solvent effects has been used for the first time to systematically explore the solvatochromic effects from solvents other than water, namely, methanol, acetonitrile, and carbon tetrachloride. For all solvents, good agreement with experimental results is observed for the solvatochromic shifts. Experimental excitation energies are reproduced with deviations of less than 0.1 eV, and shifts with respect to vacuum are in even better agreement, as they fully reproduce the solvent-dependent trends. The PE method continues to be an accurate and efficient tool also for cases where continuum models are likely to fail, e.g., when hydrogen bonding is important. The level of agreement over such diverse solvents is truly nontrivial and even better than we expected. For fairness, in relation to the much better results of the polarizable embedding QM/MM type of approach compared to the continuum approaches, it should be recalled that the continuum approach requires only a single calculation, while the QM/MM approach requires many calculations and an MD simulation for generating the structures for such calculations.

In this paper, we have shown that the inclusion of higher order multipole moments in the solvent potentials leads to faster convergence with respect to a full QM treatment. Most often, up to quadrupole moments and anisotropic polarizabilities are sufficient to cover environmental effects. The successful application of our approach to new solvents is also encouraging in relation to biomolecular studies. Most likely, the potentials can

be retrieved from ab initio calculations as demonstrated here for several solvents. First results confirm this conclusion.[24,33,60] In addition, we have shown the great potential of PE-CC to benchmark PE models on the basis of a more simplified QM description.

A good quality potential and explicit consideration of polarization effects are necessities for good results, as has been demonstrated. To improve the PE approach further, other issues of the procedure need to be addressed. The treatment of flexible molecules must be taken into account when larger (and less rigid) molecules in solution are to be considered. Additionally, the QM/MM interface might benefit from a description of Pauli repulsion and of dispersion effects at the electronic level. The documented accuracy and possibility to combine the PE model with CC approaches allows not only a systematic improvement of the QM description but that of the MM region as well. Therefore, the PE method qualifies as a reliable benchmark reference against which other methods can be assessed.

■ ASSOCIATED CONTENT

Supporting Information. All PE potentials generated for this study are listed along with the theoretical excitation energies for pyridanzine in different solvents based on different levels of theory. This material is available free of charge via the Internet at http://pubs.acs.org/.

■ AUTHOR INFORMATION

Corresponding Author
*E-mail: tschwabe@chem.au.dk.

■ ACKNOWLEDGMENT

T.S. acknowledges support through a Feodor-Lynen fellowship from the Alexander von Humboldt Foundation. O.C. and J.K. acknowledge support from the Danish Center for Scientific Computing (DCSC), the Danish national research foundation, and the Lundbeck Foundation. O.C. thanks EUROHORCs for a EURYI award.

■ REFERENCES

(1) Curtiss, L. A.; Redfern, P. C.; Raghavachari, K. *J. Chem. Phys.* **2005**, *123*, 124107.
(2) Schwabe, T.; Grimme, S. *Phys. Chem. Chem. Phys.* **2007**, *9*, 3397–3406.
(3) Goerigk, L.; Grimme, S. *J. Chem. Theory Comput.* **2010**, *6*, 107–126.
(4) Zhao, Y.; Truhlar, D. G. *Chem. Phys. Lett.* **2011**, *502*, 1–3.
(5) Frenkel, D.; Smit, B. *Understanding Molecular Simulation: From Algorithms to Applicatons*; Academic Press: San Diego, CA, 1996; Chapter 7, pp 151−176.
(6) Warshel, A.; Levitt, M. *J. Mol. Biol.* **1976**, *103*, 227–249.
(7) Klamt, A.; Schüürmann, G. *J. Chem. Soc., Perkin Trans. 2* **1993**, *2*, 799–805.
(8) Klamt, A.; Jonas, V. *J. Chem. Phys.* **1996**, *105*, 9972–9981.
(9) Cancés, E.; Mennucci, B.; Tomasi, J. *J. Chem. Phys.* **1997**, *107*, 3032–3031.
(10) Mennucci, B.; Cancés, E.; Tomasi, J. *J. Phys. Chem. B* **1997**, *101*, 10506–10517.
(11) Tomasi, J.; Mennucci, B.; Cammi, R. *Chem. Rev.* **2005**, *105*, 2999–3094.
(12) Steindal, A. H.; Ruud, K.; Frediani, L.; Aidas, K.; Kongsted, J. *J. Phys. Chem. B* **2011**, *115*, 3027–3037.
(13) Marenich, A. V.; Cramer, C. J.; Truhlar, D. G. *J. Chem. Theory Comput.* **2010**, *6*, 2829–2844.
(14) Senn, H. M.; Thiel, W. *Angew. Chem., Int. Ed.* **2009**, *48*, 1198–1229.
(15) Car, R.; Parrinello, M. *Phys. Rev. Lett.* **1985**, *55*, 2471–2474.
(16) Ohrn, A.; Karlstrom, G. *Theor. Chem. Acc.* **2007**, *117*, 441–449.
(17) Parac, M.; Doerr, M.; Marian, C. M.; Thiel, W. *J. Comput. Chem.* **2010**, *31*, 90–106.
(18) Murugan, N. A.; Jha, P. C.; Rinkevicius, Z.; Ruud, K.; Ågren, H. *J. Chem. Phys.* **2010**, *132*, 234508.
(19) Murugan, N. A.; Kongsted, J.; Rinkevicius, Z.; Ågren, H. *Phys. Chem. Chem. Phys.* **2011**, *13*, 1290–1292.
(20) Kongsted, J.; Osted, A.; Mikkelsen, K. V.; Christiansen, O. *J. Phys. Chem. A* **2003**, *107*, 2578–2588.
(21) Kongsted, J.; Osted, A.; Mikkelsen, K. V.; Christiansen, O. *J. Chem. Phys.* **2003**, *118*, 1620–1633.
(22) Nielsen, C. B.; Christiansen, O.; Mikkelsen, K. V.; Kongsted, J. *J. Chem. Phys.* **2007**, *126*, 154112.
(23) Olsen, J. M.; Aidas, K.; Kongsted, J. *J. Chem. Theory Comput* **2010**, *6*, 3721–3734.
(24) Sneskov, K.; Schwabe, T.; Kongsted, J.; Christiansen, O. *J. Chem. Phys.* **2011**, *134*, 104108.
(25) Thompson, M. A. *J. Chem. Phys.* **1996**, *100*, 14492–14507.
(26) Jensen, L.; van Duijnen, P. T.; Snijders, J. G. *J. Chem. Phys.* **2003**, *118*, 514–521.
(27) Jensen, L.; van Duijnen, P. T.; Snijders, J. G. *J. Chem. Phys.* **2003**, *119*, 3800–3809.
(28) Wesolowski, T. A.; Warshel, A. *J. Phys. Chem.* **1993**, *97*, 8050–8053.
(29) Neugebauer, J. *J. Chem. Phys.* **2007**, *126*, 134166.
(30) Day, P. N.; Jensen, J. H.; Gordon, M. S.; Webb, S. P.; Stevens, W. J.; Krauss, M.; Garmer, D.; Basch, H.; Cohen, D. *J. Chem. Phys.* **1996**, *105*, 1968–1986.
(31) Gordon, M. S.; Jensen, J. H.; Freitag, M. A.; Bandyopadhyay, P.; Stevens, W. J. *J. Phys. Chem. A* **2001**, *105*, 293–307.
(32) Arorar, P.; Slipchenko, L. V.; Webb, S. P.; Gordon, A. D. M. S. *J. Phys. Chem. A* **2010**, *114*, 6742–6750.
(33) Söderhjelm, P.; Husberg, C.; Strambi, A.; Olivucci, M.; Ryde, U. *J. Chem. Theory Comput* **2008**, *5*, 649–658.
(34) Mata, R. A. *Mol. Phys.* **2010**, *108*, 381–392.
(35) Jacob, C. R.; Neugebauer, J.; Jensen, L.; Visscher, L. *Phys. Chem. Chem. Phys.* **2006**, *8*, 2349–2359.
(36) Coutinho, K.; Canuto, S. *Adv. Quantum Chem.* **1997**, *28*, 89–105.
(37) Becke, A. D. *J. Chem. Phys.* **1993**, *98*, 5648–5652.
(38) Stephens, P. J.; Devlin, F. J.; Chabalowski, C. F.; Frisch, M. J. *J. Phys. Chem.* **1994**, *98*, 11623–11627.
(39) Dunning, T. H. *J. Chem. Phys.* **1989**, *90*, 1007–1023.
(40) Kendall, R. A.; T. H. Dunning, J; Harrison, R. J. *J. Chem. Phys.* **1992**, *96*, 6796–6806.
(41) Frisch, M. J.; Trucks, G. W.; Schlegel, H. B.; Scuseria, G. E.; Robb, M. A.; Cheeseman, J. R.; Scalmani, G.; Barone, V.; Mennucci, B.; Petersson, G. A.; Nakatsuji, H.; Caricato, M.; Li, X.; Hratchian, H. P.; Izmaylov, A. F.; Bloino, J.; Zheng, G.; Sonnenberg, J. L.; Hada, M.; Ehara, M.; Toyota, K.; Fukuda, R.; Hasegawa, J.; Ishida, M.; Nakajima, T.; Honda, Y.; Kitao, O.; Nakai, H.; Vreven, T.; Montgomery, J. A.; Peralta, J. E.; Ogliaro, F.; Bearpark, M.; Heyd, J. J.; Brothers, E.; Kudin, K. N.; Staroverov, V. N.; Kobayashi, R.; Normand, J.; Raghavachari, K.; Rendell, A.; Burant, J. C.; Iyengar, S. S.; Tomasi, J.; Cossi, M.; Rega, N.; Millam, J. M.; Klene, M.; Knox, J. E.; Cross, J. B.; Bakken, V.; Adamo, C.; Jaramillo, J.; Gomperts, R.; Stratmann, R. E.; Yazyev, O.; Austin, A. J.; Cammi, R.; Pomelli, C.; Ochterski, J. W.; Martin, R. L.; Morokuma, K.; Zakrzewski, V. G.; Voth, G. A.; Salvador, P.; Dannenberg, J. J.; Dapprich, S.; Daniels, A. D.; Farkas, O.; Foresman, J. B.; Ortiz, J. V.; Cioslowski, J.; Fox, D. J. *Gaussian 09*, Revision A.02; Gaussian, Inc.: Wallingford, CT, 2009.
(42) Gagliardi, L.; Lindh, R.; Karlström, G. *J. Chem. Phys.* **2004**, *121*, 4494–4500.

(43) Aquilante, F.; De Vico, L.; Ferré, N.; Ghigo, G.; Malmqvist, P.; Neogrády, P.; Bondo Pedersen, T. B.; Pitoňák, M.; Reiher, M.; Roos, B. O.; Serrano-Andrés, L.; Urban, M.; Veryazov, V.; Lindh, R. *J. Comput. Chem.* **2010**, *31*, 224–247.
(44) Breneman, C. M.; Wiberg, K. B. *J. Comput. Chem.* **1990**, *11*, 361–373.
(45) Jorgensen, W. L.; Maxwell, D. S.; Tirado-Rives, J. *J. Am. Chem. Soc.* **1996**, *118*, 11225–11236.
(46) Ponder, J. W. *TINKER: Software Tools for Molecular Design*, version 5.1; Washington University School of Medicine: Saint Louis, MO, 2010.
(47) Ahlström, P.; Wallqvist, A.; Engström, S.; Jönnson, B. *Mol. Phys.* **1989**, *68*, 563–581.
(48) Linse, P. *MOLSIM 3.3.0*; Lund University: Lund, Sweden, 2001.
(49) Yannai, T.; Tew, D. P.; Handy, N. C. *Chem. Phys. Lett.* **2004**, *393*, 51–57.
(50) Helgaker, T.; Jørgensen, P.; Olsen, J. *Molecular Electronic-Structure Theory*; J. Wiley: New York, 2000; Chapter 13, pp 648.723.
(51) Aidas, K. *Whirlpool*, version 1.0; University of Copenhagen: Copenhagen, 2010.
(52) DALTON, Release 2.0. See http://www.kjemi.uio.no/software/dalton/dalton.html (accessed Jan 1, 2011).
(53) Bondi, A. *J. Phys. Chem.* **1964**, *68*, 441–451.
(54) Batsanov, S. S. *Inorg. Mater.* **2001**, *37*, 871–885.
(55) Aidas, K.; Møgelhøj, A.; Nilsson, E. J. K.; Johnson, M. S.; Mikkelsen, K. V.; Christiansen, O.; Söderhjelm, P.; Kongsted, J. *J. Chem. Phys.* **2008**, *128*, 194503.
(56) Jorgensen, W. L.; Chandrasekhar, J.; Madura, J. D.; Impey, R. W.; Klein, M. L. *J. Chem. Phys.* **1983**, *79*, 926–935.
(57) Renge, I. *J. Phys. Chem. A* **2009**, *113*, 10678–10686.
(58) Baba, H.; Goodman, L.; Valenti, P. C. *J. Am. Chem. Soc.* **1966**, *88*, 5410–5415.
(59) Kongsted, J.; Mennucci, B. *J. Chem. Phys.* **2007**, *111*, 9890–9900.
(60) Rocha-Rinza, T.; Sneskov, K.; Christiansen, O.; Ryde, U.; Kongsted, J. *Phys. Chem. Chem. Phys.* **2011**, *13*, 1585–1589.